

• 临床研究 •

腰椎零回波时间成像中采样点数对图像质量影响的探讨

孙 仪¹, 徐露露¹, 吴仆射², 邹月芬^{1*}

¹南京医科大学第一附属医院放射科, 江苏 南京 210029; ²通用电气医疗, 北京 100176

[摘要] 目的: 探讨不同采样点数(number of readout points, N_{read})对腰椎零回波时间(zero echo time, ZTE)成像质量的影响, 并确定最优的 N_{read} 。方法: 招募16例健康志愿者, 分别采用128、144和160 3种 N_{read} 进行腰椎冠状位ZTE扫描, 获得 $N_{\text{read}}=128$ 、 $N_{\text{read}}=144$ 和 $N_{\text{read}}=160$ 3组图像。在各组图像中分别测量皮质骨、肌肉及松质骨区域的信号强度, 并以皮下脂肪标准差作为噪声, 计算信噪比(signal-to-noise ratio, SNR)和对比噪声比(contrast-to-noise ratio, CNR)。由2名观察者采用4分法, 从皮质骨描绘、解剖结构清晰度、感知图像噪声及总体图像质量4个方面对3组图像进行主观评价, 并采用加权Kappa检验评估观察者间评分的一致性。SNR和CNR的比较采用重复测量方差分析, 图像质量主观评分的比较采用Friedman检验, 事后分析均采用Bonferroni法。结果: 在所有测量区域(皮质骨、肌肉、松质骨)的SNR及组织间(皮质-肌肉、皮质-松质)CNR方面, $N_{\text{read}}=160 > N_{\text{read}}=144 > N_{\text{read}}=128$ (P 均 < 0.001)。在主观评价方面, $N_{\text{read}}=160$ 组明显高于 $N_{\text{read}}=128$ 组 ($P < 0.001$), 而与 $N_{\text{read}}=144$ 组间差异无统计学意义 ($P > 0.05$)。结论: 在腰椎ZTE成像中, 增加 N_{read} 有助于提升图像质量。 $N_{\text{read}}=144$ 在提供较高SNR与CNR的同时, 其主观图像质量评分与 $N_{\text{read}}=160$ 相当。综合考虑扫描时间与图像质量, 推荐将144作为腰椎ZTE成像中的最优 N_{read} 。

[关键词] 磁共振成像; 腰椎; 零回波时间成像; 骨皮质; 图像质量

[中图分类号] R445.2

[文献标志码] A

[文章编号] 1007-4368(2026)02-241-07

doi: 10.7655/NYDXBNSN251199

Exploration on the impact of the number of readout points on image quality in zeroecho time imaging of the lumbar spine

SUN Yi¹, XU Lulu¹, WU Pushe², ZOU Yuefen^{1*}

¹Department of Radiology, the First Affiliated Hospital of Nanjing Medical University, Nanjing 210029; ²GE Healthcare, Beijing 100176, China

[Abstract] **Objective:** To investigate the impact of different numbers of readout points (N_{read}) on image quality in zero echo time (ZTE) imaging of the lumbar spine, and to determine the optimal N_{read} . **Methods:** Sixteen healthy volunteers were recruited and underwent coronal ZTE scans of the lumbar spine with three different N_{read} (128, 144, and 160), to obtain three sets of images ($N_{\text{read}}=128$, $N_{\text{read}}=144$, and $N_{\text{read}}=160$). The signal intensity of the cortical bone, muscle, and cancellous bone was measured in each set, and the standard deviation of subcutaneous fat was defined as noise to calculate the signal-to-noise ratio (SNR) and contrast-to-noise ratio (CNR). Two observers subjectively evaluated the three sets of images using a 4-point scale across four aspects: cortical bone depiction, anatomical structure clarity, perceived image noise, and overall image quality. Inter-observer agreement was assessed using weighted Kappa statistics. Repeated-measures ANOVA was used to compare SNR and CNR, and the Friedman test was used to compare subjective image quality scores, with Bonferroni correction applied for post-hoc analyses. **Results:** For the SNR in all measured regions (cortical bone, muscle, and cancellous bone) and the CNR between tissues (cortical bone-muscle, cortical-cancellous bone), the results consistently showed $N_{\text{read}}=160 > N_{\text{read}}=144 > N_{\text{read}}=128$ ($P < 0.001$). In terms of subjective evaluation, the scores for the $N_{\text{read}}=160$ set were significantly higher than those for the $N_{\text{read}}=128$ set ($P < 0.001$), while the difference between the $N_{\text{read}}=160$ set and the $N_{\text{read}}=144$ set was not statistically significant ($P > 0.05$). **Conclusion:** In ZTE scanning of the lumbar spine, increasing N_{read} helps improve image quality. $N_{\text{read}}=144$ provides high SNR and CNR, and its subjective image quality scores are comparable to those of $N_{\text{read}}=160$. Considering both scanning time and image quality, 144 is recommended as the optimal N_{read} for ZTE imaging of the lumbar spine.

[Key words] magnetic resonance imaging; lumbar spine; zero echo time imaging; cortical bone; image quality

[基金项目] 国家自然科学基金(81701652)

[J Nanjing Med Univ, 2026, 46(02): 241-246, 261]

*通信作者(Corresponding author), E-mail: zou_yf@163.com (ORCID: 0000-0002-2645-1454)

磁共振成像(magnetic resonance imaging, MRI)是目前脊柱病变诊断的“金标准”^[1],能够清晰显示椎间盘退变^[2]、神经根受压及周围软组织情况^[3],在制定个性化治疗策略(如保守治疗或手术干预)中具有决定性价值^[1,4]。然而,受限于最短回波时间(echo time, TE),常规MRI序列难以显示诸如骨骼和钙化等具有超短横向弛豫时间(transverse relaxation time, T_2)的结构^[5]。相比之下,计算机断层成像(computed tomography, CT)能够更清楚地显示皮质骨结构、骨内细节及钙化灶^[6]。然而,联合使用MRI和CT会延长检查时间、增加医疗成本、延误诊疗进程,并造成解剖配准不一致和额外辐射暴露^[7-9]。为此,多项研究建议采用“类CT”、MRI作为常规MRI的补充,以实现骨骼结构的详细评估,从而尝试通过“一站式”检查完成对骨与软组织的全面评估^[9-13]。

零回波时间(zero echo time, ZTE)成像是“类CT”MRI方法的一种,可以从接近零TE开始采集快速衰减的信号,实现无辐射情况下的骨骼评估^[5]。目前,已有几项研究证实了ZTE用于诊断脊柱不同疾病的可行性,包括识别腰椎退行性改变^[14]、评估腰椎小关节和腰骶移行椎^[15]、检测多发性骨髓瘤溶骨性病变^[16]等,然而由于化学位移伪影和低翻转角导致的低信噪比(signal-to-noise ratio, SNR),腰椎ZTE图像质量不佳^[16],有待进一步优化。

既往文献已详细探讨了体素^[17]、翻转角^[18]及带宽^[19]等参数对图像质量的影响,但对于采样点数(number of readout points, N_{read})在ZTE图像中的影响仍缺乏研究。本研究在此基础上,选择合适的翻转角、体素与带宽并保持固定,通过比较不同 N_{read} 下腰椎ZTE图像的质量,系统评估该参数对成像效果的影响,以确定最优 N_{read} ,从而优化ZTE序列在腰椎成像中的应用,进一步提升图像质量。

1 对象和方法

1.1 对象

2024年12月—2025年6月在南京医科大学第一附属医院招募16例健康志愿者进行腰椎MRI扫描,其中,男9例、女7例,年龄(24.69±0.95)岁。纳入标准:①年龄>18岁;②既往无腰椎外伤史、手术史。排除标准:①存在MR检查禁忌证;②图像间存在位置移动或运动伪影。本研究经南京医科大学第一附属医院伦理委员会批准(2023-SR-700),所有志愿者均签署知情同意书。

1.2 方法

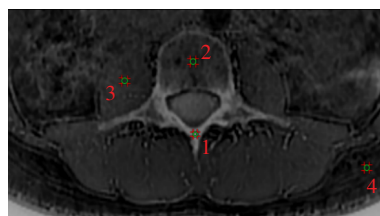
在3.0T扫描仪(Signa Premier; GE HealthCare, 美国)上,采用30通道AIR线圈和60通道脊柱线圈进行检查。受试者采取仰卧位,头先进,双手自然下垂置于身体两侧,双脚并拢并保持中立。具体扫描参数:翻转角2°,带宽±62.5 kHz,体素1 mm×1 mm×1 mm,层数100,激励次数8,分别采用128、144和160的 N_{read} 行腰椎冠状位扫描,扫描时间分别为6 min 12 s、7 min 46 s和9 min 25 s,最终获得 N_{read} -128、 N_{read} -144和 N_{read} -160 3组图像。

1.2.1 客观评价

将图像导入RadiantViewer软件中,使用软件中的多平面重建工具重建矢状位和轴位,并对图像进行灰度反转,观察者可自由调整窗宽、窗位。为定量评价3组不同 N_{read} 图像的质量,在轴位选取第3腰椎棘突与椎板连接处层面用来勾画感兴趣区(region of interest, ROI),以测量3组图像的SNR和对比噪声比(contrast-to-noise ratio, CNR),见图1。在 N_{read} -160图像上放置3 mm²的ROI,以确定皮质骨(第3腰椎棘突与椎板连接处)的信号强度(signal intensity, SI),并在同一层面分别放置2个5 mm²的ROI,以确定松质骨(椎体中心)和肌肉(右侧腰大肌)的SI。在信号均匀处、尽量避开血管和组织边界,放置5 mm² ROI测量皮下脂肪标准差(standard deviation, SD)。为确保不同 N_{read} 图像上各组ROI的大小和位置一致,减少误差,通过复制粘贴方式将 N_{read} -160图像上各组ROI复制到其他两组图像中的相同位置,以获得其他两组图像上各组织的SI及SD。测量方法如图1所示。上述SI和SD均分别测量3次,取均值后纳入公式计算。SNR和CNR计算公式如下:SNR=SI_(ROI)/SD_(皮下脂肪);CNR=[SI_(ROI)-SI_(皮质)]/SD_(皮下脂肪)。

1.2.2 主观评价

屏蔽序列信息后,随机抽取5例志愿者ZTE序列扫描图像,由2名放射科技师(观察者1、2)采用双



Numbers 1 to 4 indicate the location and extent of the regions of interest (ROI) delineated for cortical bone, cancellous bone, muscle, and subcutaneous fat, respectively.

图1 ROI勾画示意图

Figure 1 Diagram of the ROI delineation

盲法对图像进行主观评价。主观评价采用4分法,分别从皮质骨描绘^[20]、解剖结构清晰度、感知图像噪声^[8]、总体图像质量4个方面进行评分。评分标准:①皮质骨描绘(1=模糊,2=轻微模糊,3=边缘较清楚,4=边缘清晰锐利);②解剖结构清晰度(主要关注椎间孔、侧隐窝、小关节的显示,1=无法辨认,2=骨性结构边界不清,3=骨性结构边界较为清楚,4=骨性结构边界清晰可见);③感知图像噪声(1=重度,2=中度,3=轻度,4=无);④总体图像质量(1=差,2=可接受,3=好,4=优秀)。若2名观察者评分不一致,再由另1名具有10年以上工作经验的主任医师进行最终判断,确定主观评价标准。间隔2周后,2名观察者再对所有志愿者图像进行主观评价,并对评价结果做一致性检验。

1.3 统计学方法

采用SPSS 27.0软件进行统计学分析。采用加权Kappa检验评价2名观察者主观评分的一致性:0.80≤Kappa<1.00表示几乎完全一致;0.60≤Kappa<0.80表示高度一致性;0.40≤Kappa<0.60表示中等一致性;0.20≤Kappa<0.40表示一致性一般;0≤Kappa<0.20表示一致性极低。正态和非正态分布数据分别以均数±标准差($\bar{x} \pm s$)或中位数(四分位数)[$M(P_{25}, P_{75})$]表示。对ZTE序列3组不同 N_{read} (128、144、160)

图像各区域SNR、CNR的比较采用重复测量方差分析,若发现3组间差异有统计学意义,再行Bonferroni校正的两两比较;对3组图像质量主观评分的比较采用Friedman检验,若发现3组间差异有统计学意义,再行Bonferroni校正的两两比较。 $P < 0.05$ 为差异有统计学意义。

2 结果

2.1 图像客观评价结果

统计分析显示,在所有评估的解剖区域(皮质、肌肉、松质)中,SNR在3组图像间差异均具有统计学意义($P < 0.001$,表1)。事后检验显示,在皮质、肌肉和松质的SNR方面, $N_{read-160} > N_{read-144} > N_{read-128}$ ($P < 0.001$)。对于所测组织间(皮质-肌肉、皮质-松质)CNR,3组图像间差异均具有统计学意义($P < 0.001$)。事后检验显示,对于皮质-肌肉CNR和皮质-松质CNR,均有 $N_{read-160} > N_{read-144} > N_{read-128}$ ($P < 0.001$)。

2.2 图像主观评价结果

两名观察者的评分结果均显示,对于所有主观评价指标(皮质骨描绘、解剖结构清晰度、感知图像噪声、总体图像质量),3组图像间主观评分差异均具有统计学意义($P < 0.001$,表2)。事后分析显示,观

表1 3组图像间SNR和CNR的比较结果

Table 1 Comparison of SNR and CNR among the three sets of images

Objective evaluation indicator	$N_{read}(\bar{x} \pm s)$			<i>F</i>	<i>P</i>	<i>P_a</i>	<i>P_b</i>	<i>P_c</i>
	$N_{read-128}$	$N_{read-144}$	$N_{read-160}$					
SNR _{cortical bone}	29.28 ± 4.57	37.54 ± 6.12	47.56 ± 7.61	78.54	<0.001	<0.001	<0.001	<0.001
SNR _{muscle}	53.95 ± 5.98	68.61 ± 8.41	85.68 ± 10.14	100.74	<0.001	<0.001	<0.001	<0.001
SNR _{cancellous bone}	60.45 ± 8.69	79.23 ± 11.46	98.14 ± 15.52	81.09	<0.001	<0.001	<0.001	<0.001
CNR _{cortical bone-muscle}	24.67 ± 2.67	31.07 ± 4.15	38.12 ± 5.12	68.54	<0.001	<0.001	<0.001	<0.001
CNR _{cortical bone-cancellous bone}	31.17 ± 5.21	41.69 ± 5.89	50.58 ± 8.51	63.54	<0.001	<0.001	<0.001	<0.001

P_a : $N_{read-128}$ vs. $N_{read-144}$; P_b : $N_{read-128}$ vs. $N_{read-160}$; P_c : $N_{read-144}$ vs. $N_{read-160}$.

察者1的评分结果表明, $N_{read-144}$ 和 $N_{read-160}$ 两组图像各项主观评分与 $N_{read-128}$ 组间差异均具有统计学意义(P 均<0.05),观察者2的评分结果表明,对于除解剖结构清晰度外的各项评价指标, $N_{read-144}$ 和 $N_{read-160}$ 两组图像各项得分与 $N_{read-128}$ 组间差异均具有统计学意义(P 均<0.05),而在解剖结构清晰度方面, $N_{read-144}$ 和 $N_{read-128}$ 两组图像间差异没有统计学意义($P > 0.05$)。2名观察者的主观评分结果均显示,虽然 $N_{read-160}$ 组得分高于 $N_{read-144}$ 组,但两组间差异无统计学意义($P > 0.05$)。对于3组图像的各项主观评

价指标,两名观察者评分均具有高度一致性(Kappa值0.60~0.85)。ZTE序列不同组间同一层面对骨骼的显示情况见图2~4。

3 讨论

3.1 ZTE序列原理

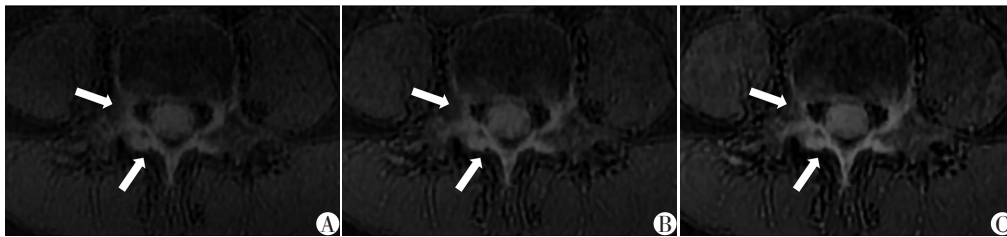
ZTE成像是一种基于三维径向K空间填充与各向同性体素采集的磁共振技术。其核心创新在于采用“先编码,后激发”的时序:在射频脉冲激发前预先施加并稳定梯度场,从而在自旋质子受激后,

表2 3组图像主观评分结果

Table 2 Subjective scoring results of the three sets of images

Subjective evaluation indicator	Observer	$N_{read}[M(P_{25}, P_{75})]$			<i>F</i>	<i>P</i>	<i>P_a</i>	<i>P_b</i>	<i>P_c</i>
		$N_{read-128}$	$N_{read-144}$	$N_{read-160}$					
Cortical bone depiction	Observer1	3(2,3)	3(3,4)	4(3,4)	25.06	<0.001	0.008	<0.001	0.752
	Observer2	2(2,3)	3(3,3)	3(3,4)	24.13	<0.001	0.011	<0.001	0.867
	Kappa	0.60(0.29,0.92)	0.79(0.52,1.00)	0.72(0.45,1.00)					
Anatomical structure sclarity	Observer1	3(2,3)	3(3,4)	4(3,4)	25.09	<0.001	0.006	<0.001	0.993
	Observer2	3(2,3)	3(3,4)	4(3,4)	19.85	<0.001	0.102	0.002	0.555
	Kappa	0.62(0.32,0.93)	0.65(0.36,0.94)	0.76(0.49,1.00)					
Perceived image noise	Observer1	2(2,3)	3(3,4)	4(3,4)	29.71	<0.001	0.001	<0.001	0.648
	Observer2	2(2,3)	3(3,3)	4(3,4)	27.44	<0.001	0.011	<0.001	0.190
	Kappa	0.72(0.41,1.00)	0.79(0.52,1.00)	0.77(0.45,1.00)					
Overall image quality	Observer1	3(2,3)	3(3,4)	4(3,4)	26.94	<0.001	0.004	<0.001	0.555
	Observer2	3(2,3)	3(3,4)	4(3,4)	22.37	<0.001	0.031	<0.001	0.648
	Kappa	0.85(0.67,1.00)	0.64(0.29,0.99)	0.69(0.37,1.00)					

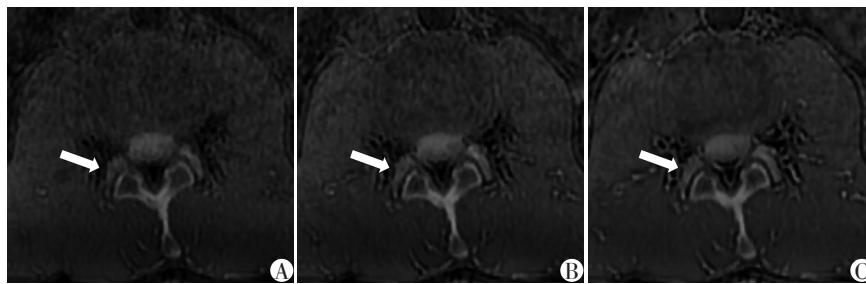
P_a: $N_{read-128}$ vs. $N_{read-144}$. *P_b*: $N_{read-128}$ vs. $N_{read-160}$. *P_c*: $N_{read-144}$ vs. $N_{read-160}$.



Images from the same volunteer obtained with N_{read} values of 128(A), 144(B), and 160(C), respectively. Compared with A, images B and C exhibit reduced image noise, resulting in clearer visualization of the lateral recess (upper arrows). The cortical bone of the pedicles and laminae also appears more distinct and sharper(lower arrows). Overall image quality scores from two observers are 2, 3, 3 and 2, 3, 4 for A, B, and C, respectively.

图2 不同 N_{read} 图像对侧隐窝同一层面骨骼显示情况的比较

Figure 2 Comparison of the visualization of bony structures at the identical level of the lateral recess among images with different N_{read}



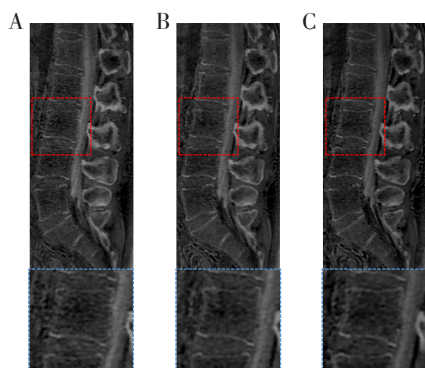
Images from the same volunteer obtained with N_{read} values of 128(A), 144(B), and 160(C), respectively. Image A exhibits noticeable noise with blurred depiction of joint spaces and intervertebral foramina. In contrast, images B and C demonstrate reduced noise and clearer delineation of these structures(arrows). Overall image quality scores from two observers are 2, 3, 4 and 2, 4, 4 for A, B, and C, respectively.

图3 不同 N_{read} 图像对小关节同一层面骨骼显示情况的比较

Figure 3 Comparison of the visualization of bony structures at the same facet joint level on images with different N_{read}

可立即通过纯频率编码方式采集其自由感应衰减信号。该设计省去了常规序列中的梯度切换环节,实现了极速的空间编码与信号采集,使TE趋近于0

(可短于 $8 \mu s$)。因此,ZTE序列能够直接捕获超短 T_2 组织的信号,为传统MRI难以显示的骨皮质等结构提供了全新的可视化手段^[5,21]。在ZTE参数中,



Images from the same volunteer obtained with N_{read} values of 128 (A), 144 (B), and 160 (C), respectively, with insets (blue boxes) showing magnified views of the L3 vertebral region (outlined in red). Image A exhibits more pronounced noise and consequently a blurred depiction of the vertebral cortex compared to B and C, which show reduced noise and superior cortical definition. Overall image quality scores from two observers are 2, 3, 4 and 2, 3, 3 for A, B, and C, respectively.

图4 不同 N_{read} 图像对正中矢状面骨骼显示情况的比较
Figure 4 Comparison of the visualization of bony structures at the mid-sagittal plane on images with different N_{read}

单个辐条(即1条K空间线)的采样点数被定义为 N_{read} , 其数值的大小与ZTE图像质量息息相关。本研究结果显示, 提高 N_{read} 可显著提高ZTE的图像质量。

3.2 SNR和CNR的提高

本研究结果表明, 与较小的 N_{read} 相比, 采用更大的 N_{read} 能够提高SNR和CNR, 原因大致如下: ZTE成像沿着径向辐条对3DK空间进行采样, 根据奈奎斯特采样定理, 所需的径向辐条数与 N_{read} 有关: 辐条数 $= \pi N_{\text{read}}^2$ [22]。在3组图像中, 随着 N_{read} 的增加, 在K空间外围进行奈奎斯特采样对应的径向辐条数增加, 继而使得K空间中心的径向辐条分布变得更加密集(K空间中心区域集中了图像的主要信号能量); 同时, K空间中心决定图像对比度, 故本研究认为 $N_{\text{read}}=160$ 具有更高的SNR和CNR。另一方面, ZTE成像重复时间(repetition time, TR)主要由读出持续时间(readout duration, T_{read})决定 [22], 随着 N_{read} 的增大, T_{read} 和TR均延长, 从而可以使组织的纵向磁化有更充分的时间恢复, 增加了每次射频激发前的纵向磁化强度, 继而提高了SNR。

3.3 图像质量主观评分的提升

相比 $N_{\text{read}}=128$ 组图像, $N_{\text{read}}=144$ 和 $N_{\text{read}}=160$ 组图像总体图像质量更佳。在图像噪声方面, $N_{\text{read}}=128$ 组图像得分最低, 而 $N_{\text{read}}=160$ 组图像得分最高, 这一点和客观结果相一致。在图像解剖结构方面, 得益于高 N_{read} 提供的高SNR和高CNR, $N_{\text{read}}=160$ 和 $N_{\text{read}}=144$

两组图像在侧隐窝、小关节和椎间孔的显示方面明显优于 $N_{\text{read}}=128$ 组图像, 这为椎间孔骨性狭窄、小关节退变等疾病的诊断提供了基础。另外, 相比传统梯度回波 (gradient echo, GRE) 序列中皮质骨和松质骨以及其他短 T_2 组织的区分能力下降 [22], ZTE成像可以提供皮质和松质间更好的对比, 这对骨骼相关疾病(如骨质疏松)的检测和管理至关重要 [8]。本研究中, 相比低 N_{read} 图像, 高 N_{read} 图像上皮质与松质、肌肉间的对比更好, 且图像噪声更小, 继而改善了对皮质骨的描绘, 这将有助于骨折等病变的检测和形态学评估, 并为椎体退行性或创伤性病变的定性或定量测量提供了良好的条件 [8]。

尽管高 N_{read} 会在一定程度上造成编码时长的延长, 引入了 T_2^* 的敏感性 [21], 但本研究显示, 随着采样点数的增加, ZTE图像仍能够提供皮质骨与松质骨间良好的对比与清晰的骨性结构边缘。可能原因如下: 一方面是由于ZTE序列中TE相比GRE序列更短, 并采用近中心起始的径向采样或其变体, 优先获取对图像CNR和SNR至关重要的K空间中心区域数据 [23]; 另一方面是序列所采用的 ± 62.5 kHz的高带宽降低了化学位移伪影和磁敏感伪影。尽管高带宽会介导SNR的降低, 但是高 N_{read} 所带来的K空间中心采集密度高、净磁化矢量大的优势可以弥补高带宽的负面效应。最后, 尽管 $N_{\text{read}}=160$ 组图像的客观评价优于 $N_{\text{read}}=144$ 组图像, 但是在主观评价方面, 二者并没有明显的差异, 说明 $N_{\text{read}}=160$ 所带来的边际效应有限, $N_{\text{read}}=144$ 所提供的影像质量和检查时间所带来的性价比更高。

3.4 局限性

①因总的扫描时间较长, 故本研究样本量较少且均在志愿者身上完成, 后续将收集更多脊柱病变患者, 以进一步证实ZTE在疾病评估中的价值。②本研究中采用次数为8的高激励次数采集, 扫描时间较长, 这是考虑到了ZTE序列中低翻转角和骨骼成像所需要的高空间分辨率可能会导致低SNR, 故选取较高的激励次数来尽可能降低图像噪声对测量的影响。③本研究仅通过优化参数来提高图像质量, 没有结合其他图像质量优化技术如深度学习, 后续将在本研究所得结论基础上结合深度学习进一步缩短扫描时间, 提高图像质量。

综上所述, 在腰椎ZTE扫描中, 增加 N_{read} 可以优化图像质量, 随着 N_{read} 的增加, SNR和CNR明显增加, 相比 $N_{\text{read}}=128$ 组图像, $N_{\text{read}}=144$ 和 $N_{\text{read}}=160$ 组图像在图像质量主观评价中表现更好。结合时间因素,

认为 N_{read} 选择144更为合适。

利益冲突声明:

全体作者均声明无利益冲突。

Conflict of Interests:

All authors declare that they have no conflict of interests.

作者贡献声明:

孙仪起草和撰写稿件,获取、分析和解释本研究的数据;徐露露设计本研究的方案,分析和解释本研究的数据,对稿件重要内容进行了修改;吴仆射分析、解释本研究的数据。邹月芬设计本研究的方案,对稿件重要内容进行了修改。

Author's Contributions:

SUN Yi drafted and wrote the manuscript, as well as obtained, analyzed and interpreted the data of this research; XU Lulu designed the research protocol, analyzed and interpreted the data of this research, and revised the important content of the manuscript; WU Pushe analyzed and interpreted the data of this research. ZOU Yuefen designed the research protocol and revised the important content of the manuscript.

[参考文献]

- [1] KIM G U, CHANG M C, KIM T U, et al. Diagnostic modality in spine disease: a review[J]. *Asian Spine J*, 2020, 14(6):910-920
- [2] 倪 婷, 徐 磊, 冯 阳, 等. 腰椎终板 Modic 改变与椎间盘退变对应关系及二者与下腰痛关系的分析[J]. *南京医科大学学报(自然科学版)*, 2019, 39(2):237-241
- NI T, XU L, FENG Y, et al. The matched association between modic changes with lumbar disc degeneration and their association with low back pain[J]. *Journal of Nanjing Medical University(Natural Sciences)*, 2019, 39(2):237-241
- [3] 秦 朗, 时 寅, 刘继永, 等. 磁共振扩散张量成像定量评估腰骶神经根压迫症[J]. *南京医科大学学报(自然科学版)*, 2018, 38(12):1715-1719
- QIN L, SHI Y, LIU J Y, et al. Diffusion tensor imaging with quantitative evaluation in lumbosacral radiculopathy [J]. *Journal of Nanjing Medical University (Natural Sciences)*, 2018, 38(12):1715-1719
- [4] ALY M M, SOLIMAN Y, ELEMAM R A, et al. How frequently MRI modifies thoracolumbar fractures' classification or decision-making? A systematic review and meta-analysis[J]. *Eur Spine J*, 2024, 33(4):1540-1549
- [5] AYDINGÖZ Ü, YILDIZ A E, ERGEN F B. Zero echo time musculoskeletal MRI: technique, optimization, applications, and pitfalls[J]. *Radiographics*, 2022, 42(5):1398-1414
- [6] TSUCHIYA K, GOMYO M, KATASE S, et al. Magnetic resonance bone imaging : applications to vertebral lesions[J]. *Jpn J Radiol*, 2023, 41(11):1173-1185
- [7] LIN Y, TAN E T, CAMPBELL G, et al. How I do it: three-dimensional MR neurography and zero echo time MRI for rendering of peripheral nerve and bone [J]. *Radiology*, 2025, 316(1):e241604
- [8] PENG L, PAN X, LIANG H, et al. Deep learning reconstruction enhances bone visualization in zero echo time MRI for cervical spondylosis: a prospective study[J]. *Eur J Radiol*, 2025, 191:112310
- [9] FERREIRA BRANCO D, BOUREDUCEN H, HAMARD M, et al. mFFE CT-like MRI sequences for the assessment of vertebral fractures[J]. *Diagnostics*, 2024, 14(21):2434
- [10] KRONTHALER S, BOEHM C, FEUERRIEGEL G, et al. Assessment of vertebral fractures and edema of the thoracolumbar spine based on water-fat and susceptibility-weighted images derived from a single ultra-short echo time scan[J]. *Magn Reson Med*, 2022, 87(4):1771-1783
- [11] WANG Q, XING X, ZHANG Z, et al. Added value of 3D fast-field-echo (FRACTURE) sequences for cervical spondylosis diagnosis: a prospective multi-reader non-inferiority study[J]. *Insights Imaging*, 2025, 16(1):114
- [12] CAFFARD T, CHIAPPARELLI E, ARZANI A, et al. Diagnosis and evaluation of cervical ossification of the posterior longitudinal ligament on zero echo time magnetic resonance imaging: an illustrative case series[J]. *Eur J Orthop Surg Traumatol*, 2024, 35(1):9
- [13] HUTCHINS J, LAGERSTRAND K, HEBELKA H, et al. Evaluation of cervical vertebral motion and foraminal changes during the spurling test using zero echo time magnetic resonance imaging and computed tomography-based micromotion analysis [J]. *Spine*, 2024, 49 (14) : E221-E228
- [14] HOU B, LIU C, LI Y, et al. Evaluation of the degenerative lumbar osseous morphology using zero echo time magnetic resonance imaging (ZTE-MRI)[J]. *Eur Spine J*, 2022, 31(3):792-800
- [15] KANIEWSKA M, KUHN D, DEININGER-CZERMAK E, et al. 3D zero-echo time and 3D T1-weighted gradient-echo MRI sequences as an alternative to CT for the evaluation of the lumbar facet joints and lumbosacral transitional vertebrae[J]. *Acta Radiol*, 2023, 64(6):2137-2144
- [16] LECOUVET F E, ZAN D, LEPOT D, et al. MRI-based zero echo time and black bone pseudo-CT compared with whole-body CT to detect osteolytic lesions in multiple myeloma[J]. *Radiology*, 2024, 313(1):e231817
- [17] AFSABI A M, LOMBARDI A F, WEI Z, et al. High-contrast lumbar spinal bone imaging using a 3D slab-selective UTE sequence[J]. *Front Endocrinol*, 2022, 12:800398
- [18] ZHAN Y, LI X, YANG X, et al. Optimization and applica-

(下转第261页)

- [17] VADHER D, ZACKEN A, SHAH V, et al. The rolling stones: a systematic review and meta-analysis of the management of gallstone ileus[J]. *Chirurgia (Bucur)*, 2024, 119(5): 483-514
- [18] LAI Y T, WU P H. Gallstone ileus[J]. *N Engl J Med*, 2022, 387(10): 924
- [19] CHUAH J S, TAN J H, KHAIRUDIN K B, et al. Case series of gallstone ileus with one-or two-stage surgery[J]. *Ann Hepatobiliary Pancreat Surg*, 2022, 26(2): 199-203
- [20] BOJAN A, PRICOP C, VLADANU M C, et al. The predictive roles of tumour markers, hemostasis assessment, and inflammation in the early detection and prognosis of gallbladder adenocarcinoma and metaplasia: a clinical study[J]. *Int J Mol Sci*, 2025, 26(8): 3665
- (收稿: 2025-09-11; 修回: 2025-12-25; 录用: 2025-12-25)
(本文编辑: 唐 震)

(上接第246页)

- tion of zero echo time sequence in MRI of sacroiliac joints: a preliminary study[J]. *Eur J Radiol*, 2026, 194: 112505
- [19] WIESINGER F, SACOLICK L I, MENINI A, et al. Zero TEMR bone imaging in the head[J]. *Magn Reson Med*, 2016, 75(1): 107-114
- [20] ENSLE F, KANIEWSKA M, LOHEZIC M, et al. Enhanced bone assessment of the shoulder using zero-echo time MRI with deep-learning image reconstruction[J]. *Skeletal Radiol*, 2024, 53(12): 2597-2606
- [21] WEIGER M, PRUESSMANN K P. MRI with zero echo time[M]. Chichester: John Wiley & Sons, Ltd, eMagRes, 2012, 1(2): 311-321
- [22] WIESINGER F, HO M L. Zero-TE MRI: principles and applications in the head and neck[J]. *Br J Radiol*, 2022, 95(1136): 20220059
- [23] 李绍林, 洪 楠. MR超短/零回波时间技术在骨骼肌肉系统中的应用现状与未来展望[J]. *中国医学影像技术*, 2025, 41(8): 1273-1279
- LI S L, HONG N. MR ultrashort and zero echo time in musculoskeletal system: current application status and future perspectives[J]. *Chin J Med Imaging Technol*, 2025, 41(8): 1273-1279
- (收稿: 2025-10-31; 修回: 2026-01-06; 录用: 2026-01-06)
(本文编辑: 唐 震)